Journal of Zhejiang University-SCIENCE A (Applied Physics & Engineering)
ISSN 1673-565X (Print); ISSN 1862-1775 (Online)
www.jzus.zju.edu.cn; www.springerlink.com
E-mail: jzus@zju.edu.cn

Effect of heat-treatment on LiZn ferrite hollow microspheres prepared by self-reactive quenching technology*

Xu-dong CAI[†1], Jian-jiang WANG[2], Xiao-jun JIANG[1], Jun LING[1], Yi XU[1], Zhan-tong GAO[3]

[1]*The First Scientific Research Institute of Wuxi, Wuxi 214035, China*

[2]*The Seventh Department, Mechanical Engineering College, Shijiazhuang 050003, China*

[3]*Cadres Office, Mechanical Engineering College, Shijiazhuang 050003, China*

[†]E-mail: caixudong87@qq.com

Received Dec. 8, 2016; Revision accepted Sept. 12, 2017; Crosschecked Mar. 23, 2018; Published online Apr. 10, 2018

Abstract: Lithium-zinc ferrite hollow microspheres (LiZn FHMs) containing special surface crystals were synthesized by self-reactive quenching technology. The samples were heat-treated at 1200 °C and held for 4 h. The influence of the heat-treatment on LiZn FHMs was studied. The results show that the surface of hollow microspheres is smooth without heat-treatment. The phase components are Fe_2O_3, Fe_3O_4, $Li_{0.435}Zn_{0.195}Fe_{2.37}O_4$, and $Li_{0.5}Fe_{2.5}O_4$. The minimum reflectivity is −13.5 dB, and the corresponding frequency is 7.5 GHz. The effective absorption band lower than −10 dB is 6.2–8.5 GHz, and the bandwidth is 2.3 GHz. After heat-treatment, crystals on the surface of hollow microspheres grow significantly. Multiple-shape micro-nano crystals containing triangular, polygonal, and irregular crystal are generated. However, the phase composition does not change. The real part of the permittivity (ε'), the imaginary part of permittivity (ε''), the real part of permeability (μ'), and the imaginary part of permeability (μ'') all increase, and the microwave absorption properties at low frequency are significantly increased, with the absorption peak moving to a lower frequency range. The minimum reflectivity is −26.5 dB, and the corresponding frequency changes to 3.4 GHz. The effective absorption band is 2.6–4 GHz, and the bandwidth is 1.4 GHz.

Key words: LiZn ferrites; Heat-treatment; Low frequency; Microwave absorption properties
https://doi.org/10.1631/jzus.A1600768 **CLC number:** TB333

1 Introduction

Stealth technology has seen rapid development in the weapons systems of countries around the world over past decades and represents one of the major breakthroughs in military technology since World War II. It has been listed as a basic element of "competition strategy". Radar absorbing materials are important applications of this technology (Zhang et al., 2007; Yin et al., 2013). However, most studies have concentrated on high-frequency absorbents (8–20 GHz), and research on low-frequency absorbents, lower than 8 GHz, is scarce (Qu, 2009; Xie et al., 2010; Feng et al., 2013). This is responsible for the lack of large wavelength absorbents (Sun, 2007; Tong et al., 2012).

LiZn ferrites are absorbents widely used in the 0.5–8 GHz range, and have been extensively studied (Xia et al., 2010). Some researchers have synthesized LiZn ferrites and investigated their microwave absorption properties (Yu et al., 2007; Jiang et al., 2010). Gruskova et al. (2008) studied absorption properties of LiZn ferrites substituted by Ti, Bi, and Mn. However, LiZn ferrites have disadvantages including large density and poor matching thickness, and their low frequency absorption properties are difficult to control (Liu et al., 2007). Thus, it is hard to

* Project supported by the National Natural Science Foundation of China (No. 51172282) and the Hebei Provincial Natural Science Foundation of China (No. E2015506011)
ORCID: Xu-dong CAI, https://orcid.org/0000-0003-4492-6983

meet the need for novel stealthy materials which are "thin, light, wide, and strong". From previous research (Cai et al., 2015a), it can be concluded that hollow microspheres have a series of advantages such as large specific area, low density, and great microwave absorption properties. In this study, self-reactive quenching technology developed by our team is applied to prepare LiZn ferrites with hollow structures, in order to obtain absorbents with low density and fine microwave absorption properties in the low frequency band.

Because of the super large subcooled temperature of self-reactive quenching technology, surface crystals of LiZn ferrite hollow microspheres (FHMs) are difficult to fully grow (Cai et al., 2013). As a result, hollow microspheres containing pure phases cannot be obtained, and the microwave absorption properties below 8 GHz are hard to effectively control. Cai et al. (2013) found that, after applying appropriate heat-treatment technology, the growth of surface crystals of LiZn ferrites may be promoted and the content of target phases is improved. In addition, the microwave absorption properties of LiZn ferrites in the low frequency band can be effectively adjusted by controlling the microstructure. This will be beneficial for exploring absorbents at low frequency.

In this study, self-reactive quenching technology integrating heat-treatment technology is applied to obtain LiZn FHMs with special surface crystals. The effects of heat-treatment on morphology, phase components, and microwave absorption properties in low frequency band are investigated, in order to obtain an absorbent with fine microwave absorption properties.

2 Experimental

Fe powders, Li_2CO_3 powders, Zn powders, Fe_2O_3 powders, sucrose (precursor of C, 50 g), epoxy resin (bonding agent, 50 ml), and Bi_2O_3 powders (fluxing agent, 2% in weight) were chosen. Reaction (a) shows the stoichiometry ratio of main reactive system. The quantities of ZnO and O_2 are defined as k and x, respectively. According to (Lan et al., 2007; Sun and Sun, 2007), the values of k and x are selected as 0.4 and 0.3, respectively. Agglomerate powders are obtained as follows:

$$\begin{aligned}&0.5(2.5-0.5x-2k)Fe_2O_3+2kFe+xZnO\\&\quad+0.25(1-x)Li_2CO_3+1.5kO_2\\&\quad\rightarrow 0.25(1-x)CO_2+Li_{0.5-0.5x}Zn_xFe_{2.5-0.5x}O_4.\end{aligned}\tag{a}$$

Firstly, the materials mentioned above were put into a ball mill (LJM-5L type, Tianjin Taisete, China), and anhydrous ethyl alcohol was added as the medium and steel balls were added to grind for 6 h. Secondly, epoxy resin and alcohol were mixed into solution, and then they were put into the mill to stir grind for 2 h. Thirdly, the mixtures were dried at 80 °C in the oven in order to evaporate ethyl alcohol. Then they were carbonized at 150 °C in the oven until no smoke was released. After that, they were comminuted by disintegrator (FW177 type, Tianjin Taisete, China). Finally, agglomerate powders with the particle size of about 40 μm were obtained to spray after the sieving process. The spraying distance was 400 mm.

Cai et al. (2015b) provided the chemical reactions for preparing LiZn FHMs as shown in Reactions (b)–(g), which are the decompositions of Reaction (a). In addition, the adiabatic combustion temperature (T_{ad}) of Reaction (a) is 1985 K. It is concluded that when $T_{ad}\geq 1800$ K, self-propagation high-temperature synthesis (SHS) reactions can take place (Yang, 2010). Thus, the reactions of preparing LiZn FHMs are the SHS reactions:

$$3Fe+2O_2\rightarrow Fe_3O_4,\tag{b}$$

$$4Fe_3O_4+O_2\rightarrow 6Fe_2O_3,\tag{c}$$

$$Li_2CO_3\rightarrow Li_2O+CO_2,\tag{d}$$

$$Li_2O+5Fe_2O_3\rightarrow 4Li_{0.5}Fe_{2.5}O_4,\tag{e}$$

$$ZnO+Fe_2O_3\rightarrow ZnFe_2O_4,\tag{f}$$

$$\begin{aligned}&(1-x)Li_{0.5}Fe_{2.5}O_4+xZnFe_2O_4\\&\quad\rightarrow Li_{0.5-0.5x}Zn_xFe_{2.5-0.5x}O_4.\end{aligned}\tag{g}$$

Fig. 1 shows the preparation diagram of LiZn FHMs. The detailed processes and mechanisms have been described in a previous report of our research team (Cai et al., 2015c). Then LiZn FHMs were heat-treated in a resistance furnace (GST-10-1400, Tianjin Taisete, China) at 1200 °C with the heating rate of 240 °C/min and then held for 4 h.

The morphology of samples was observed by a scanning electron microscope (SEM) (QUANTA FEG-250, FEI Company, USA). The phase structures were characterized by BRUKER D2 PHASER X-ray

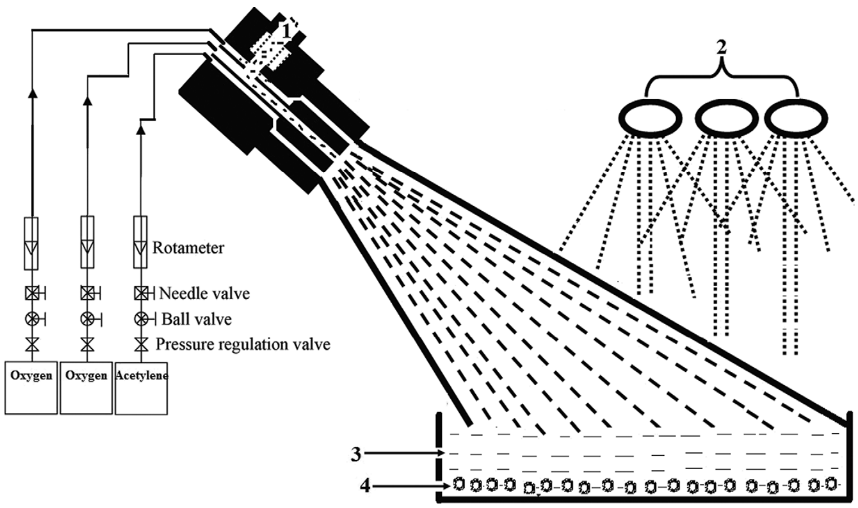

Fig. 1 Principle diagram for preparation of LiZn FHMs by self-reactive quenching technology
1: agglomerate powders; 2: water spraying system; 3: cooling medium (distilled water); 4: hollow ceramic microspheres

diffraction (XRD) (Cu Ka, λ=0.1542 nm). The density of LiZn FHMs was determined by the Archimedes method.

For the measurement of microwave absorption properties, LiZn FHMs were homogeneously dispersed in paraffin with a weight ratio of LiZn FHMs-to-paraffin of 3:2. The mixture was formed into a toroidal specimen through a coaxial mould, with outer and inner diameters of 7.00 and 3.04 mm, respectively. Complex permittivity ($\varepsilon=\varepsilon'-j\varepsilon''$) and complex permeability ($\mu=\mu'-j\mu''$) were measured by the Vector Network Analyzer (Agilent-N5242A, USA) in the frequency range of 0.5–18 GHz. ε' is the real part of the permittivity, ε'' is the imaginary part of permittivity, μ' is the real part of permeability, and μ'' is the imaginary part of permeability.

According to the theory of transmission lines (Lou, 2014), the microwave absorption properties can be calculated as the reflectivity (R).

$$R = 20\lg\left|\frac{Z_{\text{in}}-1}{Z_{\text{in}}+1}\right|, \quad (1)$$

$$Z_{\text{in}} = \left(\frac{\mu}{\varepsilon}\right)\tanh\left[\text{j}\left(\frac{2\pi fd}{C}\right)\left(\frac{\mu}{\varepsilon}\right)^{1/2}\right], \quad (2)$$

where Z_{in} is the input impedance of absorbent samples, d is the thickness of the absorbent sample, f is the frequency of the incident electromagnetic wave, and C is velocity of light in free space.

3 Results and discussion

Figs. 2a–2c illustrate SEM images of the products without heat-treatment, and Figs. 2d–2f show SEM images after being heat-treated at 1200 °C. As shown in Figs. 2b and 2c, the quenching products are hollow structures. According to Figs. 2a–2c, it is indicated that LiZn FHMs without heat-treatment are composed of closed spherical particles, single-hole spherical particles, and porous spherical particles, as well as a few irregular non-spherical particles. The surface morphology of LiZn FHMs consists of a smooth type and a rough type. No crystals appear on the surface of the smooth type. A few crystals can be seen on the surface of rough type but the crystal growth is not obvious.

After heat-treatment, the smoothness of LiZn FHMs decreases and crystals have grown dramatically. Multi-shape micro and nano crystals containing triangular, polygon, and irregular crystals are formed, with a distribution between 800 nm and 15 μm. As shown by arrow 1 in Fig. 2e, nano-crystals with "stepped structure" are formed on the surface of LiZn FHMs. The lowest surface energy principle (Zhang and Zhang, 1981) shows that the corresponding morphology represents an equilibrium state if the surface energy is the lowest in isovolumetric and thermostatic conditions. Atomic close-packed planes in the crystals have the lowest surface energy, and if atomic closed-packed planes are crystal planes, the crystals are most stable. After heat-treatment, the crystal growth on the surface of LiZn FHMs is not uniform, so the outer surface of crystals and the atomic close-packed planes are not parallel. In order to maintain the lowest energy of the surface, crystals with "bench structure" are formed and the bench planar surfaces are crystal surfaces which have the lowest surface energy (Hu et al., 2010).

It is found that the densities of LiZn FHMs are 1.95 g/cm^3 and 1.86 g/cm^3 before and after heat-treatment, respectively, using the Archimedes method. However, the destiny of $Li_{0.435}Zn_{0.195}Fe_{2.37}O_4$ solid powder is 3.26 g/cm^3 (Liu et al., 2008). Thus, it is indicated that LiZn FHMs are solid structures, and this is beneficial for obtaining light-weight absorbents.

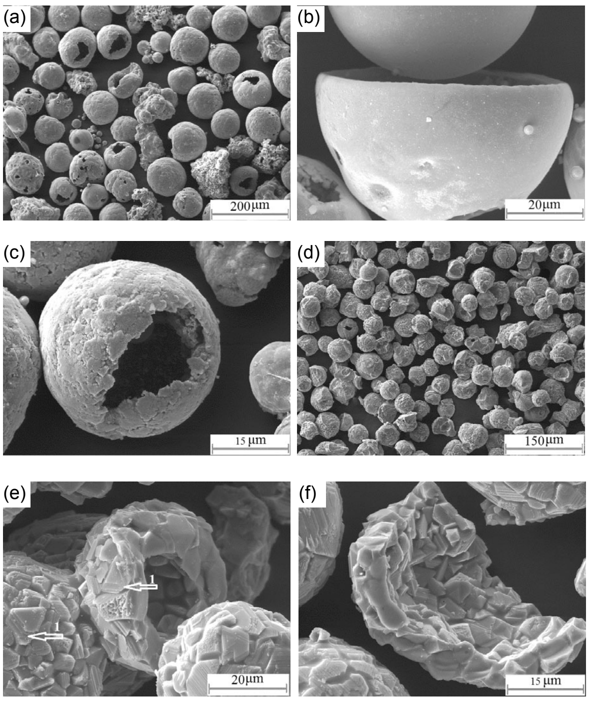

Fig. 2 SEM photographs of LiZn FHMs before (a)–(c) and after heat-treatment (d)–(e)

Fig. 3 displays the XRD patterns before and after heat-treatment. It is indicated that phase components have not changed after heat-treatment. They are still composed of Fe_3O_4, Fe_2O_3, $Li_{0.435}Zn_{0.195}Fe_{2.37}O_4$, and $Li_{0.5}Fe_{2.5}O_4$. $Li_{0.35}Zn_{0.3}Fe_{2.35}O_4$ has not been found in the phase components. This may be caused by the characteristics of self-reactive quenching technology used in this study. Complex chemical reactions take place when particles fly into the flaming field, so $Li_{0.35}Zn_{0.3}Fe_{2.35}O_4$ cannot be obtained. However, $Li_{0.435}Zn_{0.195}Fe_{2.37}O_4$ appears instead. $Li_{0.435}Zn_{0.195}Fe_{2.37}O_4$ can be seen as $(Li_{0.54}Fe_{0.46})_{0.805}Zn_{0.195}Fe_2O_4$, which has a spinel structure and has similar properties to $Li_{0.35}Zn_{0.3}Fe_{2.35}O_4$. In addition, the intensity of the diffraction peak has increased after heat-treatment. It is indicated that crystallization is more obvious, in correspondence with the obvious crystal growth shown in the SEM images of Fig. 2b.

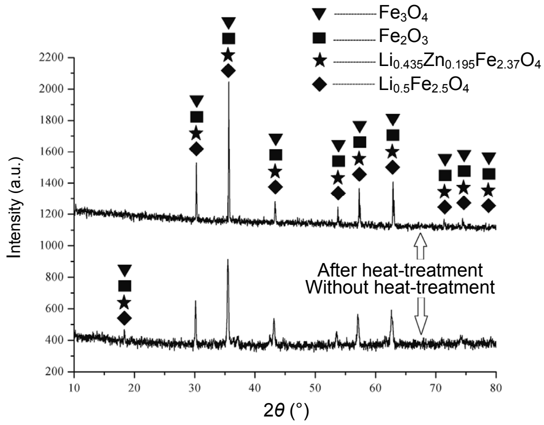

Fig. 3 XRD patterns of LiZn FHMs before and after heat-treatment

Fig. 4 shows the frequency dependence of relative complex permittivity and permeability of LiZn FHMs before and after heat-treatment. It can be concluded that the real part of permittivity (ε') changes little with the increase of frequency without heat-treatment. The imaginary part (ε'') increases slowly from 0.2 to 1.3. The real part of complex permeability (μ') decreases from 1.6 to 0.9 with the increase of frequency. The imaginary part (μ'') increases from 0.51 to 0.58 and then decreases from 0.58 to 0.08.

After heat-treatment, ε' increases significantly and its variation range is from 10.7 to 13.6. ε'' increases in the range from 1.1 to 3.4. The significant increase of ε' and ε'' may be associated with the formation of multiple-shape micro-nano crystals, which makes the effect of space charge polarization stronger. The appearance of multiple-shape micro-nano crystals results in the contact ways among the LiZn FHMs transforming from point-contact to surface-contact and line-contact. Conducting networks are

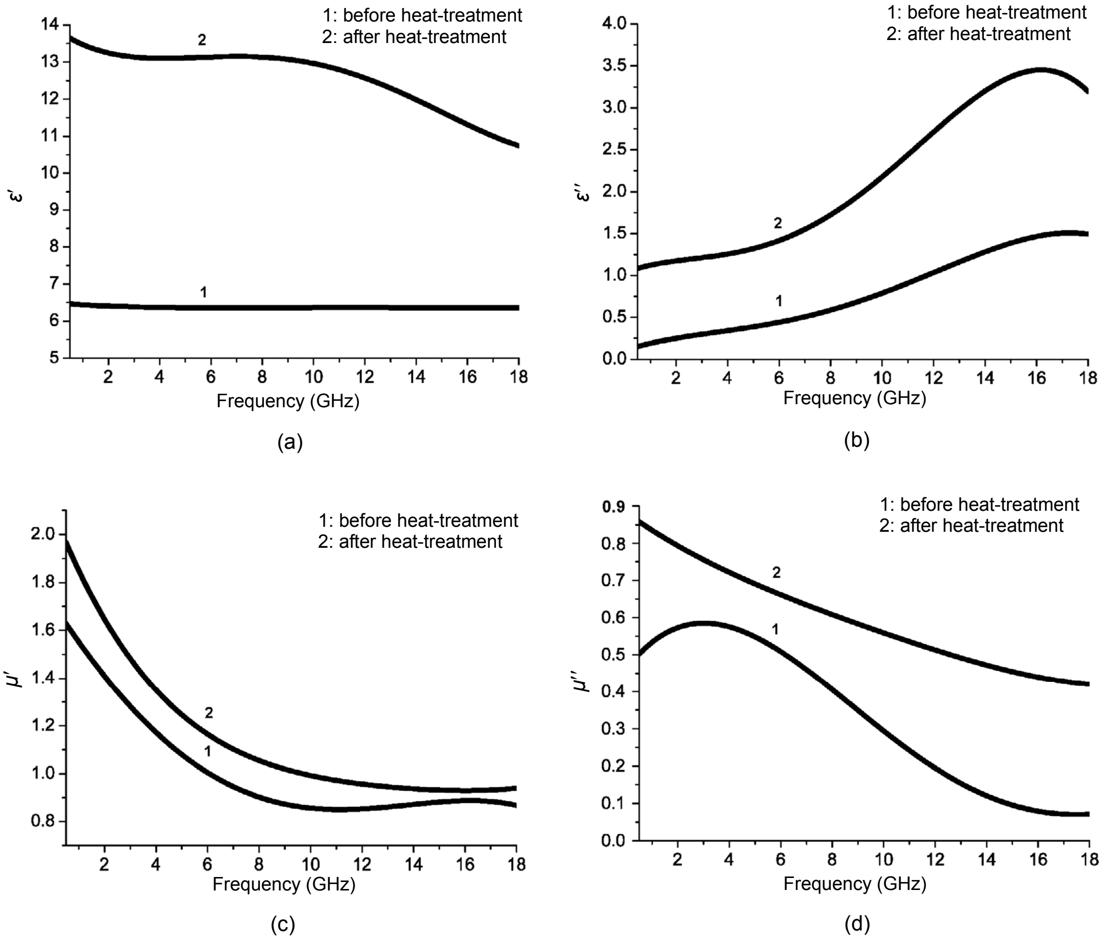

Fig. 4 Four electromagnetic parameters of LiZn FHMs before and after heat-treatment
(a) ε'; (b) ε''; (c) μ'; (d) μ''

easy to form, and electron transitions in the microscopic structures of hollow microspheres are amplified (Si and Dong, 2006; Cai et al., 2015c). As a result, dielectric loss is improved. The real part of the complex permeability (μ') and the imaginary part of the complex permeability (μ'') both increase after heat-treatment compared with those before heat-treatment. This conclusion is in accordance with that of Yu et al. (2015). The increase of permeability may be ascribed to the increase of the natural resonance effect, and the detailed reasons are as follows. The surface of hollow microspheres shows multiple-shape micro-nano crystals containing triangular, polygonal, and irregular crystals after heat-treatment, and these have high shape anisotropy and magnetic anisotropy. Hollow microspheres undergo the interaction of alternating magnetic field incidence and the effective field of magneto-crystalline anisotropy. When the frequency of the two fields is equal, resonance will occur. LiZn FHMs can absorb electromagnetic waves dramatically.

The reflectivity of LiZn FHMs absorbent samples with the thickness of 3 mm before and after heat-treatment is shown in Fig. 5. From the figure, it is indicated that the microwave absorption properties of LiZn FHMs have changed significantly after heat-treatment. For the sample without heat-treatment, the minimum reflectivity reaches −13.5 dB at 7.5 GHz and the effective frequency bandwidth ($R<-10$ dB) is 2.3 GHz (6.2–8.5 GHz). The minimum reflectivity reaches −26.5 dB at 3.4 GHz and the effective frequency bandwidth is 1.4 GHz (2.6–4 GHz) for the sample after heat-treatment. These data show that the minimum reflectivity decreases obviously and the

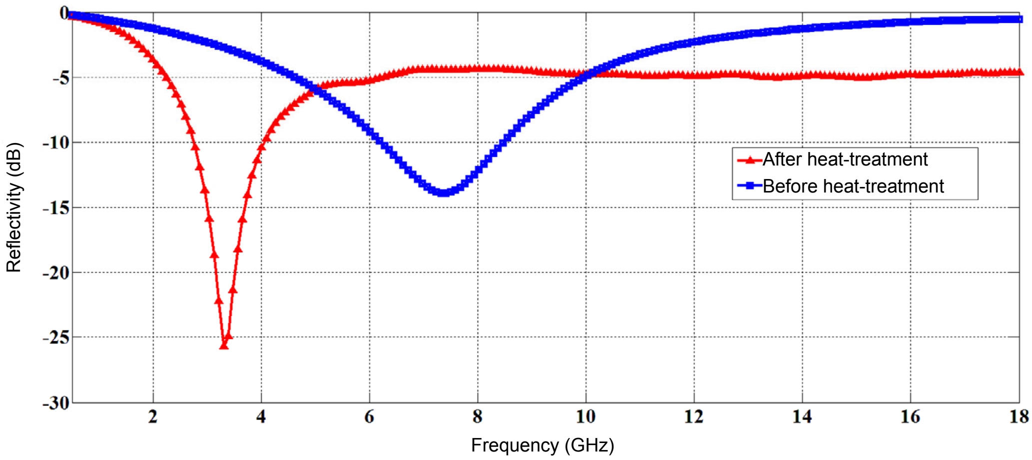

Fig. 5 Reflectivity of LiZn FHMs absorbent samples with the thickness of 3 mm before and after heat-treatment

absorbing peak transforms to low frequency for the heat-treated sample. Consequently, the microwave absorption properties are improved dramatically after heat-treatment in respect of the minimum reflectivity and absorption peak. This may be the result of several factors, including density and porosity. However, the main cause may be the appearance of multiple-shape micro-nano crystals containing triangular, polygonal, and irregular crystals. Significant crystal growth occurs. Thus, the loss mechanisms of the electromagnetic wave change greatly, the contacting ways among LiZn FHMs increase significantly, and the coupling ways are diverse (Liu and Guo, 2002). LiZn FHMs are filled with paraffin where waves can get through easily, so large numbers of intermediate couplings and complex couplings are formed. As a result, the loss of the electromagnetic waves is bound to increase (Zan et al., 2009). Moreover, electromagnetic waves are absorbed when going into the conducting wall of hollow microspheres by impedance matching without heat-treatment. They are absorbed again when reaching the other conducting wall. However, due to the apparent crystal growth on the surface of LiZn FHMs after heat-treatment, the electromagnetic wave loss is enhanced between two conducting walls. A significant crystal growth on the internal surface appears. Consequently, a lot of reflection and scattering of electromagnetic waves take place when they are oscillating in the cavity of hollow microspheres, and electromagnetic waves are further absorbed.

4 Conclusions

LiZn FHMs are synthesized by self-reactive quenching technology based on a $Fe+Zn+Fe_2O_3+O_2+Li_2CO_3$ reactive system. Then the samples were calcined at 1200 °C for 4 h. The surface morphology, phase components, and microwave absorption properties before and after heat-treatment were studied. The surface of LiZn FHMs is smooth and crystal growth is not obvious without heat-treatment. After heat-treatment, crystals on the surface of LiZn FHMs grow significantly. Multiple-shape micro-nano crystals containing triangular, polygonal, and irregular crystals are generated. These crystals are distributed between 800 nm and 15 μm. In addition, four electromagnetic parameters of LiZn FHMs all increase, the microwave absorption properties are improved and the absorption peak transforms to a lower frequency range. The minimum reflectivity reaches −26.5 dB at 3.4 GHz and the effective frequency bandwidth is 1.4 GHz (2.6–4 GHz). The appearance and growth of multiple-shape micro-nano crystals may be the main reasons for improvement of microwave absorption properties at low frequency after heat-treatment.

References

Cai XD, Wang JJ, Xu BC, et al., 2013. Effect of heat-treatment temperature on structure and microwave electromagnetic properties of hollow multiphase ceramic microspheres. *Journal of the Chinese Ceramic Society*, 41:1331-1338 (in Chinese).

Cai XD, Wang JJ, Liang GH, et al., 2015a. Effect of $NaNO_3$ foaming agent on barium ferrite hollow microspheres prepared by self-reactive quenching technology. *Journal of Alloys and Compounds*, 636:348-356. https://doi.org/10.1016/j.jallcom.2015.02.015

Cai XD, Wang JJ, Yang RX, et al., 2015b. Influence of the foaming agent on the particle size and microwave absorption properties of hollow ceramic microspheres. *International Journal of Applied Ceramic Technology*, 12: E8-E16. https://doi.org/10.1111/ijac.12171

Cai XD, Wang JJ, Xu BC, et al., 2015c. Preparation of LiZn ferrites hollow microspheres based self-reactive quenching technology and study on their low-frequency microwave absorption properties. *Rare Metal Materials and Engineering*, 391:2335-2339.

Feng YB, Tang CM, Qiu T, 2013. Effect of ball milling and moderate surface oxidization on the microwave absorption properties of FeSiAl composites. *Materials Science and Engineering: B*, 178(16):1005-1011. https://doi.org/10.1016/j.mseb.2013.06.004

Gruskova A, Slama J, Dosoudil R, 2008. Microwave properties of some substituted LiZn ferrites. *Journal of Magnetism and Magnetic Materials*, 320(20):e860-e864. https://doi.org/10.1016/j.jmmm.2008.04.131

Hu GX, Cai X, Rong YH, 2010. Fundamentals of Materials Science. Shanghai Jiao Tong University Press, Shanghai, China, p.20-22 (in Chinese).

Jiang H, Guo Z, Zhao L, et al., 2010. Preparation and microwave absorption properties of LiZn ferrite. *Journal of Inorganic Materials*, 25(1):73-76. https://doi.org/10.3724/SP.J.1077.2010.00073

Lan YH, Gao XX, Bao XQ, 2007. Study of barium ferrite based on self-propagating high-temperature synthesis. *Materials Review*, 21:333-335.

Liu CY, Lan ZW, Jiang XN, et al., 2008. Effects of sintering temperature on the microstructure and magnetic properties of LiZn ferrites. *Journal of Magnetism and Magnetic Materials*, 39:36-38.

Liu SH, Guo HJ, 2002. Electromagnetic shielding and wave-absorbing materials. *Journal of Functional Materials and Devices*, 8:213-216.

Liu SH, Liu JM, Dong XL, 2007. Electromagnetic Wave Shielding and Absorbent. Chemical Industrial Press, Beijing, China, p.67-70 (in Chinese).

Lou HF, 2014. Designing, Synthesis and Study on High-frequency Absorbing Performance of Ferrite Hollow Microspheres by Self-reactive Quenching Technology. MS Thesis, Mechanical Engineering College, Shijiazhuang, China (in Chinese).

Qu LY, 2009. Preparation and properties of low frequency band absorbing material. *Modern Defense Technology*, 37:131-133.

Si Q, Dong FQ, 2006. Study on electromagnetic shielding effectiveness in low frequency of coatings doping aggregate and iron carbonyl. *Functional Materials*, 37: 883-892.

Sun C, 2007. Synthesis and Microwave Absorbing Properties of Low Frequency Absorber. MS Thesis, Shandong University, Jinan, China (in Chinese).

Sun C, Sun KN, 2007. Preparation and characterization of magnesium-substituted LiZn ferrites by a sol-gel method. *Physical Review B*, 391:335-338.

Tong SY, Wu JM, Tung MJ, et al., 2012. Effect of Ni concentration on electromagnetic wave absorption of (Ni, Mn, Zn)Fe_2O_4/resin particulate composites. *Journal of Alloys and Compounds*, 525:143-148. https://doi.org/10.1016/j.jallcom.2012.02.093

Xia DG, Lu BS, Wang HK, 2010. Preparation Principle and Technology of Soft Magnetic Ferrites. Shaanxi Press, Xi'an, China, p.325-327 (in Chinese).

Xie GZ, Yuan LK, Wang P, et al., 2010. GHz microwave properties of melt spun Fe-Si alloys. *Journal of Non-crystalline Solids*, 356(2):83-86. https://doi.org/10.1016/j.jnoncrysol.2009.10.007

Yang M, 2010. Technology Handbook of Heat-treatment. China Machine Press, Beijing, China, p.124-126 (in Chinese).

Yin C, Stark B, Chen YQ, et al., 2013. Adaptive minimum energy cognitive lighting control: integer order vs fractional order strategies in sliding mode based extremum seeking. *Mechatronics*, 23(7):863-872. https://doi.org/10.1016/j.mechatronics.2013.09.004

Yu J, Chen SJ, Chen X, et al., 2015. Experimental investigation on mechanical properties and permeability evolution of red sandstone after heat treatments. *Journal of Zhejiang University-SCIENCE A (Applied Physics & Engineering)*, 16(9):749-759. https://doi.org/10.1631/jzus.A1400362

Yu Z, Chen DZ, Lan ZW, et al., 2007. Effect of Bi_2O_3 on properties of LiZn ferrites. *Journal of Inorganic Materials*, 22:1173-1177.

Zan MSD, Kato I, Ab-Rahman MS, et al., 2009. Characterization of a-Si:H/SiN multilayer waveguide polarization using an optical pumping application-LED. *Journal of Zhejiang University-SCIENCE A*, 10(10):1421-1427. https://doi.org/10.1631/jzus.A0820327

Zhang KC, Zhang LH, 1981. Crystal Growth. Science Press, Beijing, China, p.232-233 (in Chinese).

Zhang ZQ, Li TH, Jing DQ, 2007. Present status and perspectives of the radar absorbing material. *Materials Review*, 21:307-310.

中文概要

题　目： 热处理对自反应淬熄法制备低频 **LiZn** 铁氧体空心微珠的影响

目　的： 自反应淬熄法制备的 LiZn 铁氧体空心微珠密度小，低频吸波性能良好，但微珠表面晶型生长不

充分。对其采用特定热处理工艺不仅可以使晶体充分发育，获得特定晶型，还可以实现对低频吸波性能的有效调控。本文旨在研究热处理工艺对LiZn铁氧体空心微珠表面形貌、相结构和低频吸波性能的影响。

创新点： 1. 通过热处理工艺，实现对 LiZn 铁氧体空心微珠表面形貌、相结构和低频吸波性能的有效调控；2. 深入分析热处理工艺对 LiZn 铁氧体空心微珠低频吸波性能的改善机理。

方　法： 1. 通过工艺探索，确定热处理的详细工艺参数。2. 通过扫描电子显微镜检测和 X 射线衍射分析，获得热处理前后 LiZn 铁氧体空心微珠的微观形貌（图 2）和物相组成（图 3）。3. 通过矢量网络分析仪，获得热处理前后材料的电磁参数（图 4）；在此基础上对比其吸波性能（图 5），并研究吸波影响机理。

结　论： 1. 采用 240 °C/min 升温至 1200 °C 并保温 4 h 的热处理后，LiZn 铁氧体空心微珠表面晶粒明显长大；2. 热处理后，微珠四个电磁参数均有所增大，低频吸波性能明显提高，吸收峰值向低频移动；3. 表面多种形状微纳米晶粒的形成和长大可能是 LiZn 铁氧体空心微珠低频吸波性能得以提高的主要原因。

关键词： LiZn 铁氧体；热处理；低频；吸波性能